

Overcurrent Relays Coordination Considering Transient Stability Study of Induction Generator Using a Method Based on Terminal Voltage

AmirHossein Taheri Jam^{1,*}, Reza Mohammadi chabanloo¹, Ehsan Bagherzadeh¹, Hossein Askarian Abyaneh², Mojtaba Nasiri²

¹ Electrical Engineering Department, Shahid Beheshti University, Tehran, Iran

² Department of Electrical Engineering, Amirkabir University of Technology, Tehran, Iran

ARTICLEINFO

ABSTRACT

Article history:

Received 18 August 2022

Received in revised form 07 October 2022

Accepted 14 November 2022

Keywords:

Induction generator

Transient stability

Grid fault

OCR coordination

Genetic algorithm

Nowadays, with increasing penetration of Induction Generators (IG) in the electricity grid, it is of great importance that IG be connected to the grid in the fault conditions. In this paper, a terminal voltage based method for transient stability study of IG is proposed. For this purpose, an improved analytical method is used to determine Critical Clearing Time (CCT) of IG in the state of grid fault, including near and non-near faults. For the faults occurring far from the terminal of generator, electromagnetic torque is not equal to zero during fault. Hence, equivalent circuit model of IG and network is used to calculate the CCT. A new formulation based on terminal voltage of IG is presented to consider the stability constraint on Over Current Relay (OCR) coordination, to prevent disconnecting of IG in grid fault condition. Simulations are carried out on two samples network, and the results demonstrate the efficiency of proposed method.



Copyright: © 2022 by the authors. Submitted for possible open access publication under the terms and conditions of the Creative Commons Attribution (CC BY) license (<https://creativecommons.org/licenses/by/4.0/>)


1) Introduction

In recent years, the use of new renewable energy has grown rapidly and among the renewable energy sources, wind power with Induction Generator (IG) is a more interesting choice to develop. Hence, the penetration level of IG in the grid has been increased. As a result, the transient stability of them is an important issue for

continuous operation of grid [1]. In the previous works, transient stability analysis for fault near IG and its impact on IG characteristics have been studied [1-6]. Appropriate model for squirrel cage IGs (SCIG), including single-squirrel cage and double-squirrel cage IGs, is proposed for rotor speed stability studies [2]. The authors of [3] and [4] have studied equivalent model of a wind farm for

* Corresponding author

E-mail address: amirhoseintaherijam@gmail.com

 <https://www.orcid.org/0009-0000-2065-4114>

<http://dx.doi.org/10.52547/ijrtei.1.1.10>

transient stability studies using dynamic simulation. The effect of network parameters on transient stability of wind farm has been studied in [5]. Also, in [6], the transient analysis of IG at unbalanced fault has been performed and it has been compared with that of IG at balanced fault.

The authors of [7] have proposed a trial and error method using dynamic simulation to determine CCT, which involves several repetitive runs. CCT is the stability criteria in the generator transient stability. Hence, CCT estimation problem has been solved with dynamic simulation, which avoids repetitive runs [8-10]. Also, methods for determining CCT with terminal voltage and rotor speed have been studied and have been compared with each other in [11].

The methods based on iterative analysis in the time domain have been proposed to determine CCT of IGs [12-14]. In [13], the transient stability of multi IG network has been studied for fault in different places of network. This method, which is based on step by step calculation, uses IG equivalent circuit and Norton equivalent model of network. In [14], Lyapunov function and controlling unstable equilibrium point (CUEP) have been obtained to calculate CCT using step by step time domain integration. An analytical method for transient stability of IG has been proposed only for fault in the terminal of IG in [15]. Also, the effect of IG parameters on transient stability has been investigated in the study.

Transient Stability of Dual Stator-Winding Induction Generator (DWIG) is studied in [28]. This paper improves transient stability by using slip frequency control containing braking resistors.

CCT calculation for doubly fed induction generator (DFIG) has been studied in [16]. In fault condition, crowbar protection acts to protect the rotor and convertor during the fault. When the crowbar protection is activated, DFIG action will be as same as IG with crowbar resistance connecting to the rotor side. So in this condition, DFIG can be analyzed by IG studies.

Also improving transient stability of DFIG is studied in [29], [30]. In [29] bridge fault current limiter used for reducing power transient stability of DFIG. In [30] investigate the influence of the closed-loop control system on transient stability

In [17] has been investigated CCT calculation for synchronous generator in presence multi induction generator. IGs were modeled as negative loads for CCT calculation of synchronous generator and stability of IGs were not considered.

Presence of renewable energy sources in distribution networks can associate problem for protection systems that overcurrent protection is one of them. In the result, some authors have been investigated overcurrent protection with renewable energy sources [18-20]. In [18], the authors solved over-current coordination problem by using fault current limiter (FCL) selection in

presence of distributed generation (DG). Also in [19], has been improved coordination equivalents for distribution feeders with renewable generation.

In recent years, the modern grid code enforces the wind generators to remain connected to the grid in fault conditions [21]. This ability is known as low voltage ride through (LVRT). If the wind generator disconnects from the grid, it may be lost the active power generation after clearing the fault. In the previous works, setting of the generator bus relays has been determined considering CCT for faults at the generator terminal [22]. The contribution of IG to fault current and its impact on OCR coordination has been studied in [23]; however, the stability of IG has not been considered.

In this paper, an improved analytical method proposed for CCT calculation of IG in the state of grid fault. This method is based on the equivalent model of IG and network in three states: pre-fault, during fault and post-fault. After sensitivity analysis on the network parameters, a simplified method is derived for determining the CCT of IG per voltage sag in the terminal of IG. Two important application of this model in stability study of IG is presented; improving LVRT and considering stability constraint in OCR coordination. In fact, the contribution of this paper to earlier work includes three novelties as below:

- CCT calculation with considering non-zero electromagnetic torque of IG during grid fault
- Deriving a new formulation for CCT per voltage sag
- Considering the stability constraint of IG in OCR coordination algorithm using terminal voltage based method

The proposed method with related equations is fully described in the following.

2) Transient Stability of IG

In order to explain the transient stability of IG, a test network is considered as shown in Fig. 1(a). This test network consists of an IG with 2MVA capacity connected to a 2.4 kV, 50 Hz network [12].

It is supposed that a fault occurs in line 2. Fig. 1(b) shows torque-slip curve of IG in pre-fault and during fault states. As can be seen, during fault condition, electrical torque of IG reduces because of voltage sag, however, speed of mechanical torque variation is slower than electrical torque variation, so mechanical torque remains almost unchanged. For this reason, rotor speed increases, and the rotor slip starts to change from initial slip. Transient stability of IG depends on the clearing time of fault. IG will remain stable, if the fault is cleared before that rotor speed reaches to critical speed. As shown in Fig. 1(b), initial slip (s_i) and critical slip (s_c) can be obtained from intersection of electrical and mechanical curves.

Fig. 1(c) shows the torque-speed curves of IG when the fault is cleared by tripping the circuit breakers of line 2.

In this state, network structure alters, hence, electromagnetic torque and critical slip (s_c) are changed.

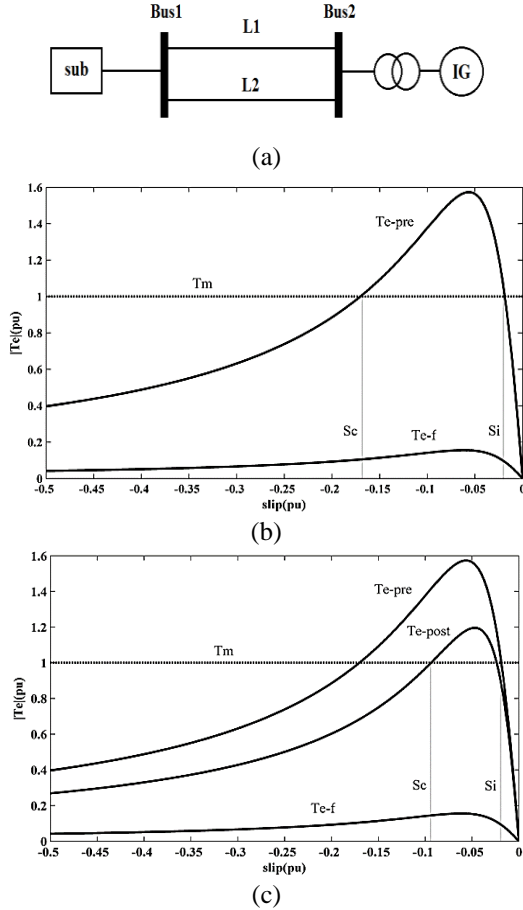


Fig. 1. Test network consists of IG. (a) Single line diagram of test network. (b) Torque-angle curve without changing in network structure in post-fault. (c) Torque-angle curve with tripping L2 in post-fault.

CCT calculation has been studied previously by assuming that fault occurs in the generator terminal [15]. In this condition, electromagnetic torque is equal to zero during fault and CCT is the linear function of slip. Relation between electrical torque and rotor slip can be given by:

$$\frac{ds}{dt} = -\frac{dw}{dt} = -\frac{1}{2H}(T_e - T_m) \quad (1)$$

Using (1) yields:

$$dt = \frac{2H}{T_m - T_e} ds \quad (2)$$

By integrating Eq. (2) from initial slip to critical slip, CCT is obtained as:

$$CCT = 2H \int_{s_i}^{s_c} \frac{ds}{T_m - T_e} \quad (3)$$

For fault in the terminal of the generator, T_e is equal to zero, and T_m is constant during fault. So, Eq. (3) is simplified as follows:

$$CCT = \frac{2H}{T_m}(s_c - s_i) \quad (4)$$

3) CCT Determining of IG For Non-near Fault

In non-near fault condition, the electromagnetic torque cannot be considered equal to zero, during fault, and Eq. (3) cannot be simplified as Eq. (4). In the other word, for CCT calculation using Eq. (3), the electromagnetic torque, during fault, should be obtained as a function of rotor slip. For this purpose, circuit modeling of IG is developed and used to calculate the electromagnetic torque.

3.1) Extended Circuit Model of IG

The model of IG is extended by considering network equivalent circuit and capacitor bank. As shown in Fig. 2(a), U_s and Z_s are the voltage and impedance equivalent of the network, respectively, and X_c is the reactance of the parallel capacitor bank. $R_s + jX_s$ and $R_r/s + jX_r$ are the stator and rotor side impedance, respectively, and X_m is the magnetizing reactance of IG. $s = 1 - \omega_r$ is the rotor slip, which ω_r is the rotor speed. Equivalent circuit is simplified as shown in Fig. 2(b). Where U_{th} and Z_{th} are thevenin equivalent values for voltage and impedance, respectively, which are seen from rotor side.

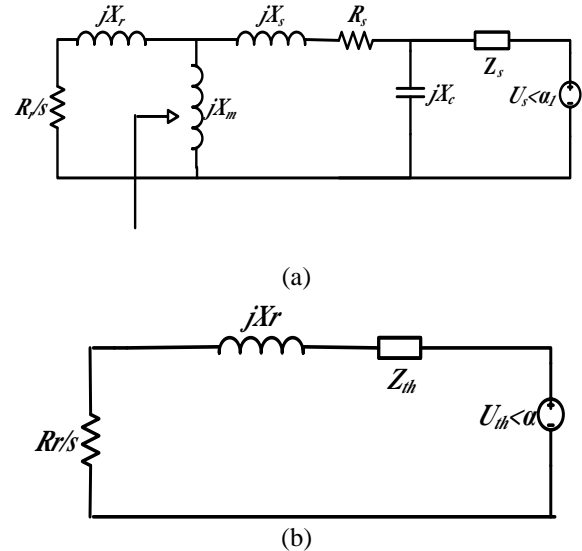


Fig. 2. Equivalent circuit of IG. (a) Complete equivalent circuit. (b) simplified equivalent circuit.

According to the simplified equivalent circuit of IG, rotor current I_r is calculated:

$$I_r = \frac{U_{th}}{\sqrt{\left(\frac{R_r}{s} + R_{th}\right)^2 + (X_r + X_{th})^2}} \quad (5)$$

The electrical torque T_e can be determined as follows:

$$T_e = \frac{R_r}{s} I_r^2 \quad (6)$$

So, substituting Eq. (5) into Eq. (6), after some simplifications yields:

$$T_e = \frac{s}{as^2 + bs + c} \quad (7)$$

Where a, b and c are as below:

$$a = \frac{R_{th}^2 + (X_r + X_{th})^2}{R_r U_{th}^2}, \quad b = \frac{2R_{th}}{U_{th}^2}, \quad c = \frac{R_r}{U_{th}^2} \quad (8)$$

Electrical torque is obtained as a function of rotor slip in Eq. (7). This equation can be used to draw the torque-slip curve of IG as shown in Fig. 1 in three states: pre-fault, during fault and post-fault. Since, the parameters a, b and c are the functions of network thevenin voltage (U_s) and network thevenin impedance (Z_s), the torque-slip curve is different for three mentioned states.

CCT can be determined substituting Eq. (7) into Eq. (3) as below:

$$\begin{aligned} CCT &= \frac{2H}{T_m} \int_{s_i}^{s_c} \left(1 + \frac{\frac{1}{T_m} s}{as^2 + (b - \frac{1}{T_m})s + c}\right) ds \\ &= \frac{2H}{T_m} (s_c - s_i) + \frac{2H}{T_m} \int_{s_i}^{s_c} \left(\frac{\frac{1}{T_m} s}{as^2 + (b - \frac{1}{T_m})s + c}\right) ds \end{aligned} \quad (9)$$

In Eq. (9), a, b and c are the parameters of torque-slip curve in the state of during fault, according to Eq. (7). Also, the parameters of torque-slip curve in pre-fault and post-fault states should be calculated to determine the initial slip (s_i) and critical slip (s_c), respectively.

3.2) Extended Circuit Model of IG

To calculate the CCT using Eq. (9), thevenin equivalent circuit of network, including thevenin voltage and thevenin impedance should be determined in three states: pre-fault, during fault and post-fault [23].

3.2.1 Thevenin Voltage

Thevenin voltage at the terminal of IG is equal to bus voltage without connecting of IG to the network. Bus voltage in pre-fault and post-fault states, can be determined using load flow calculations. In during fault condition, the bus voltage is determined using fault calculation analysis. When a fault occurs at bus f of a network with m buses, the voltage of all buses is obtained from fault analysis equation as follows [24]:

$$\begin{bmatrix} \Delta U_1 \\ \vdots \\ \Delta U_n \\ \vdots \\ \Delta U_m \end{bmatrix} = \begin{bmatrix} Z_{11} & \dots & Z_{1m} \\ Z_{21} & \dots & Z_{2m} \\ \vdots & \ddots & \vdots \\ Z_{m1} & \dots & Z_{mm} \end{bmatrix} \begin{bmatrix} 0 \\ \vdots \\ I_f \\ \vdots \\ 0 \end{bmatrix} \quad (10)$$

Where ΔU_i is the voltage deviation between pre-fault and during fault conditions. Z is the impedance matrix of network, including Z_{11} to Z_{mm} , and also, I_f is the fault current which is calculated as below:

$$I_f = \frac{U_f^{(pre-f)}}{Z_{ff}} \quad (11)$$

Where $U_f^{(pre-f)}$ is the pre-fault voltage of bus f. Therefore, the voltage at the bus n which the IG is installed, in during fault, can be calculated substituting Eq. (11) into Eq. (10) as below:

$$U_n^{(fault)} = U_n^{(pre-f)} - Z_{nf} \left(\frac{U_f^{(pre-f)}}{Z_{ff}}\right) \quad (12)$$

3.2.1 Thevenin Impedance

Thevenin impedances at the bus n, in pre-fault and post-fault states are equal to the diagonal elements (Z_{nn}) of Z. Thevenin impedance in during fault is equal to Z'_{nn} in fault condition. Importing the fault in impedance matrix, Z changes to Z' which can be obtained easily by inverting the admittance matrix of network considering the fault.

$$Z' = (Y')^{-1} \quad (13)$$

3.3) Stability of IG per Terminal Voltage

3.3.1 CCT-VS Characteristic

As mentioned in the previous section, values of a, b and c are the functions of network thevenin voltage (U_s) and network thevenin impedance (Z_s) during fault. So the second part of Eq. (9) is a function of network parameters while, the first part is independent of them. Hence, Eq. (9) can be considered as below:

$$CCT = A + f(U_s, Z_s) \quad (14)$$

Where f (U_s, Z_s) and A are:

$$f(U_s, Z_s) = \frac{2H}{T_m} \int_{s_i}^{s_c} \left(\frac{\frac{1}{T_m} s}{a_2 s^2 + (b_2 - \frac{1}{T_m})s + c_2}\right) ds \quad (15)$$

$$A = \frac{2H}{T_m} (s_c - s_i) \quad (16)$$

Since, in the fault condition, thevenin impedance of network is very smaller than generator impedance, voltage drop caused by thevenin impedance can be neglected. To clarify this fact, in Fig. 3(a) the CCT values of IG is obtained using Eq. (9). It can be seen, assuming a constant U_s , the CCT value of IG is approximately constant to different thevenin impedances. The variation range of Z_s is between 0 and 0.02 ohm for fault in different points of simple network.

Since, the MVA capacity of IG should be in the allowable range for interconnecting to a network, the short circuit impedance in point of common coupling, which is equal to Z_s , is very smaller than generator impedance. On the other hand, the value of Z_s during fault is lower than it's value in pre-fault condition (0.02 ohm). Hence, neglecting of Z_s during fault condition is an acceptable approximation in all usual networks. So, Eq. (14) can be written as follows.

$$CCT = A + f(U_s) \quad (17)$$

The first part (A) is the CCT of IG when the fault is occurred in the terminal of IG and the terminal voltage become to zero, as studied in the previous works. It can be seen from Eq. (16), the value of A depends on the installing point of IG in the network which determines S_c and S_i , and is independent of fault location.

Solving Eq. (17), considering test network parameters given in [11], the CCT formulation per terminal voltage can be determined as follows:

$$CCT = \left[\begin{array}{c} 0.56 \times U_s^2 \times k_1(U_s) \times \text{Arctan} \left[\frac{k_1(U_s)}{k_2(U_s)} \right] \\ 2.13s + \frac{\quad}{k_2(U_s)} \\ -0.28 \times U_s^2 \times \log(s \times k_1(U_s) + s^2 + 0.006) \end{array} \right]_{s_i}^{s_c} \quad (18)$$

$$k_1(U_s) = 0.03 + 0.26 \times U_s^2 \quad (19)$$

$$k_2(U_s) = \sqrt{0.02 - 0.01 \times U_s^2 - 0.07 \times U_s^4} \quad (20)$$

Asymptote of CCT's curve determined by root of $K_2(U_s)$ function. According to the Eq. (17), CCT is obtained as a function of U_s and CCT- U_s curve that is shown in Fig. 3(b) for maximum and minimum of Z_s . Note that U_s is terminal voltage of IG in the fault condition. The curve has asymptote between 0.71 and 0.73 for variation of Z_s between maximum and minimum of it's rang. This voltage is a critical voltage for stability (CVS), and generator will remain stable if U_s is greater than CVS.

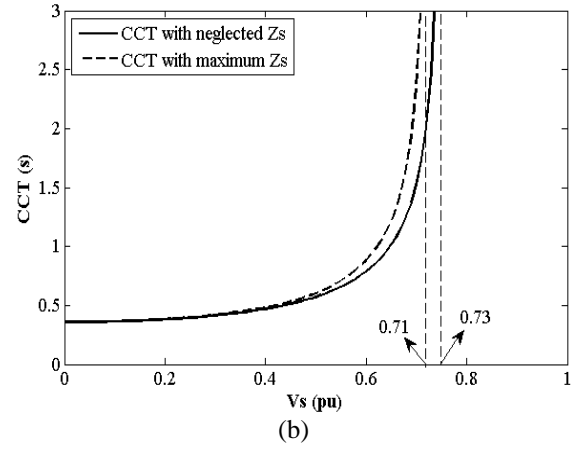
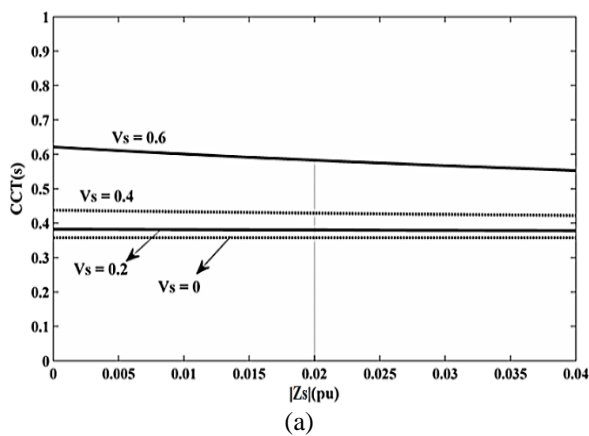


Fig. 3. (a) CCT versus thevenin impedance for different thevenin voltages. (b) CCT versus thevenin voltage for maximum and minimum thevenin impedance.

The curve of Fig. 3(b) can be determined for any IG, which depends on the installation point of IG in the network. So, CCT can be calculated for fault in different points of network and with different fault resistance only by determining voltage sag in the terminal of the generator.

3.3.2 OCR Coordination Considering CCT

With increasing the capacity of IGs in the network, it is important to stay them in the network for avoiding of inappropriate outages. Hence, the setting of relays in the distribution network can be modified to clear the grid fault before instability of IG. The proposed method using CCT- V_s curve can be applied to determine the CCT of IG for the fault in different point of the network. In order to achieve this goal, in this section, OCR coordination is studied by considering CCT.

Coordination of relays is carried out using GA which is a powerful artificial optimization technique [25-27]. In optimal coordination of OCR the decision variables which should be determined are Time Dial Setting (TDS) of relays. To achieve a better result in OCR coordination algorithm considering CCT of IG, the pickup current of relays (I_p) also are considered as decision variables. The performance of I_p in keeping the stability of IG is fully described in next section. The common objective function for optimal OCR coordination is as below:

$$\text{Minimized: } OF = \sum_{i=1}^N (t_i) \quad (21)$$

$$\text{Subject to: } t_i - t_j \geq CTI_1 \quad \forall (i, j) \in \Omega \quad (22)$$

$$TDS_i^{\min} \leq TDS_i \leq TDS_i^{\max}, \quad I_p^{\min} \leq I_p \leq I_p^{\max} \quad (23)$$

Where t_i is the operating time of i^{th} relay for the fault near to the relay and Ω is the set of main and backup relay pairs. t_i and t_j are the operating times of main and backup relays, respectively, for the fault near to the main relay. Furthermore, CTI_1 is the coordination time interval between main and backup relays which is assumed equal to 0.25.

The time interval between the relay operating time and the CCT of IG should be greater than CTI_2 to consider the delay of circuit breaker opening and safety margin. So, the second constraint is formulated as below:

$$CCT(fault(X, R)) - t_i(fault(X, R)) \geq CTI_2 \quad fault(X, R) \in S_i \quad (24)$$

Where t_i and CCT , respectively, are the operating time of i^{th} relay and the CCT of IG, for the fault in the X percent of the protected line with the resistance R. S_i is the set of all three-phase faults occur along the protected line with different fault resistances. CTI_2 is assumed to be 0.2 sec. in this paper.

Since, the coordination algorithm using GA needs numerous iterations, calculation of Eq. (26) for all mentioned faults in each iteration will cause to large run time. In the other hand, many of the faults in a line with different resistances cause to similar voltage sag in the terminal of IG and lead to similar CCT. Therefore, Eq. (24) is rewritten using CCT-US curve. The relation between fault current (I_f) and terminal voltage of IG can be written from Eq. (10) as below:

$$U_k = VU_k(0) - Z_{k(n+1)}I_f \quad (25)$$

Where bus k is installing point of IG and $n+1$ is a new bus created to consider fault point on the line. The operating time of OC relay is a function of fault current and following popular time-current characteristic is considered:

$$t_i(I_f) = \left(\frac{A}{\left(\frac{I_f}{I_b}\right)^p} + B \right) TDS \quad (26)$$

The parameters A, B and p are constants that vary with the type of used characteristic. Substituting Eq. (25) into Eq. (26) yields the operating time of relay as a function of IG terminal voltage (U_k).

$$t_i(V_k, Z_{k(n+1)}) = \left(\frac{A}{\left(\frac{V_k(0) - U_k}{Z_{k(n+1)}}\right)^k} + B \right) TSM \quad (27)$$

If the protected line is assumed between bus n and m, considering the relation between impedance parameters $Z_{kn} \leq Z_{k(n+1)} \leq Z_{km}$, Eq. (27) can be considered with Z_{km} , instead of calculating all operating times of relay with changing the fault location on the line.

$$t_i(U_k) = \left(\frac{A}{\left(\frac{U_k(0) - U_k}{Z_{km}}\right)^k} + B \right) TSM \quad (28)$$

CCT-US curve can be compared easily with the operating time of relay using (28). So, Eq. (24) can be rewritten as Eq. (29):

$$CCT(U_k) - t_i(U_k) \geq CTI_2 \quad (29)$$

4) Simulation and Results

4.1) Simple Network

The first sample system to verify the method is a 10kv and 50Hz network with 1MVA capacity IG connected via a transformer, as shown in Fig. 4. The network parameters are given in Appendix.

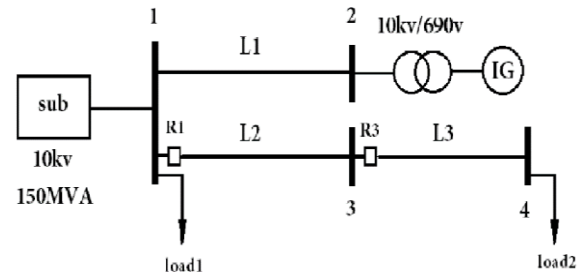


Fig. 4. Single line diagram of simple network.

4.1.1 Stability of IG for Grid Fault

The CCT of IG for fault over the line L2 (in Fig. 4) is given in Table I. In third column, CCT is calculated using a new analytical method by Eq. (9). As can be seen, the CCT value increases for faults occurring farther from the generator. To validate the result of new method, CCT determined by simulation in Simulink/MATLAB and the results are given in second column of Table I. It can be seen; the results of proposed analytical method have acceptable deviation (maximum 3.1%) compare to simulation method results.

The last column shows the voltage sag in the terminal of IG for faults occurring in line L2. According to section 2, part C, CCTs are determined from CCT-US curve by using voltage sag, and the results are given in the last column of Table II. As can be seen, maximum deviation compared to simulation method is 4.54 percent.

Table I. CCT result of new method for simple network during fault on line L2.

Fault distance from bus1 (pu)	Simulation method	New method (Eq. 9)	Simplified method using Voltage sag (Eq. 17)	
	CCT (ms)	CCT (ms)	Deviation (%)	Voltage of IG (pu)
0	360	357	0.83	0
0.1	375	367	2.13	0.09
0.2	385	376	2.34	0.16
0.3	400	390	2.50	0.23
0.4	420	407	3.10	0.28
0.5	439	426	2.96	0.33
0.6	460	447	2.83	0.37
0.7	485	470	3.09	0.41
0.8	505	495	1.98	0.44
0.9	530	521	1.70	0.47
1	550	539	2.00	0.50

4.1.2 OCR Coordination Considering CCT

After CCT calculation, the coordination of relays R1 and R3 are studied in Fig. 4 considering the stability of IG. According to coordination constraint in Eq. (22), the time interval between operating time of backup relay (R1) and main relay (R3) for the fault close to R3 should be equal to $CTI_1=0.25$. Since, the time setting and operation

characteristic of relay R3 is assumed to be $TDS_3=0.05$ and extremely inverse, respectively, the operating time of relay R1 for the fault close to R3 is obtained 0.27 sec.

Then, time setting of R1 (TDS_1) can be calculated considering three standard characteristics, including normally, very and extremely inverse. Fig. 5(a) shows this three characteristics of relay R1 and the CCT curve versus the fault location in line L2 (without considering fault resistance).

IG will remain stable for fault in L2, if the operating time of R1 is smaller than CCT. In the other word, the stability constraint of Eq. (24) should be satisfied. According to the Fig. 5(a), the minimum time intervals between the curves of CCT and relay operating time by using NI, VI and EI characteristics are obtained 0.13, 0.23 and 0.28, respectively. Therefore, very and extremely inverse curves can be used for R1 to keep the stability of IG. But the NI curve does not satisfy the stability constraint even by changing the TDS of relay. If the TDS of relay is reduced to satisfy the stability constraint, the operating time of relay R1 will decrease and the coordination of relay R1 and R3 will be disturbed. So, selecting the suitable characteristics of relays is required to achieve better results.

Since, the OCR characteristic selection has some limitations, the pickup current selection is the other solution which is used for this problem, as shown in Fig. 5(b). It can be seen, for fixed relay characteristic (assumed NI) the slope of relay curve increases by enhancement of pickup current. If I_p is selected lower than 600A, time interval between CCT and operating time of R1 will be lower than 0.2 sec. So, I_p should be selected higher than 600A to satisfy both of stability and coordination constraints. It is suggested that, in greater networks the optimization algorithm based on GA is used for determining TDS and I_p , simultaneously.

The curves of figures 5(a) and 5(b) are considered without fault resistance. To consider all faults with all resistances along the protected line, as described in section 4.3, the curves of operating time of relays and CCT of IG are obtained versus terminal voltage of IG. These curves are shown in Fig. 5(c). It can be seen that by selecting NI characteristic of relay, $I_p=600A$ and $TDS=0.1$, the time interval between two curves is greater than $CTI_2=0.2$. This result also obtained from Fig. 5(b).

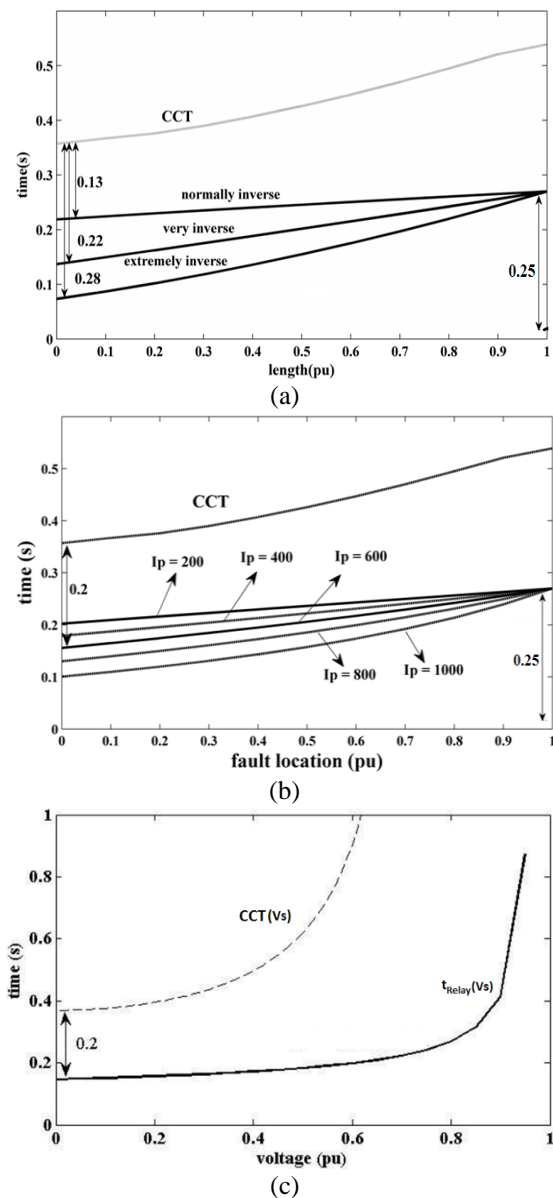


Fig. 5. Operating time of R1 and CCT for fault along line L2. (a) Considering various characteristic type of relay (without fault resistance). (b) Considering various relay pickup current (without fault resistance). (c) Operating time of R1 and CCT versus terminal voltage of IG (U_s).

4.2) IEEE 30 Bus Network

The proposed method also has been applied to IEEE 30 bus network, which is a meshed sub-transmission/distribution system. The distribution section of the network that will be studied here is fed from three primary distribution substations 132/33 kV at buses 1, 6 and 13, as shown in Fig. 6. The information of network is given in [24]. Also, one IG has been installed at bus 10 that its information is given in Appendix.

4.2.1 Stability of IG for Grid Fault

The CCTs are calculated for three-phase faults in different buses of network using the proposed method, as given in Table II. It can be seen; the stability of IG will be disturbed for fault in five buses of network. To validate

the proposed method, CCTs also are obtained using simulation method in Simulink/MATLAB. The calculation result of CCT using two methods, is approximately similar with the maximum deviation of 3.05% percent, for five mentioned buses.

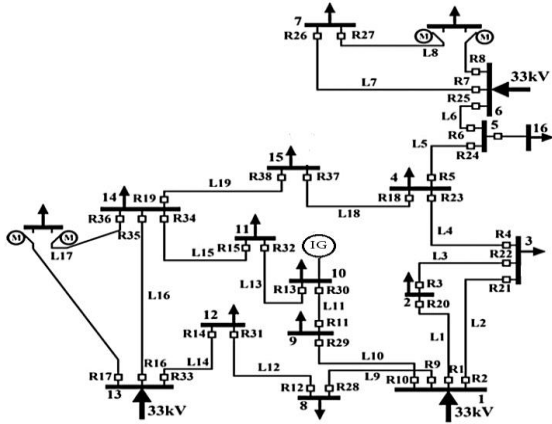


Fig. 6. Single line diagram of IEEE 30-bus distribution network.

Table II. CCTs for IEEE 30 bus system for fault in different buses.

Bus number	Simulation method CCT(ms)	Proposed method CCT(ms)	Deviation (%)
1	450	460	2.22
2	Stable	Stable	-
3	Stable	Stable	-
4	Stable	Stable	-
5	Stable	Stable	-
6	Stable	Stable	-
7	Stable	Stable	-
8	Stable	Stable	-
9	425	412	3.05
10	400	404	1.00
11	465	478	2.79
12	Stable	Stable	-
13	Stable	Stable	-
14	740	748	1.08
15	Stable	Stable	-

4.2.2 OCR Coordination Considering CCT

OCR coordination algorithm based on GA, as represented in section 3, is used to determine the OCR settings. Values of I_p and TDS is optimized in this algorithm. The range of TDS is considered between 0.05 and 2, and the range of I_p is assumed to be between 0.5 and 2.5 times of the nominal current. Also, characteristic of OCRs is assumed to be IEC extremely inverse curve. The proposed method is applied to network in two states; without considering CCT (stability constraint) and with considering CCT. In the state one, only coordination constraint according to Eq. (22), between all main and backup relays is considered to be satisfied. The result of

TDS and I_p is given in Table III. In the state two, in addition to the coordination constraint, stability constraint according to Eq. (29) is satisfied.

Table III. OCR coordination result for TDS and I_p of relays.

Relay Num.	without considering CCT		With Considering CCT		Relay Num.	without considering CCT		With Considering CCT	
	TDS	I_p	TDS	I_p		TDS	I_p	TDS	I_p
1	0.45	437	0.19	747	20	0.51	103	0.19	191
2	0.14	403	0.24	347	21	0.25	100	0.31	100
3	0.51	281	0.22	494	22	0.26	380	0.33	399
4	0.21	423	0.73	249	23	0.46	219	1.56	142
5	0.13	474	0.86	201	24	0.35	188	0.35	227
6	0.07	395	0.93	117	25	0.09	615	0.08	721
7	0.12	322	0.81	103	26	0.17	100	0.07	100
8	0.16	170	0.39	110	27	0.05	329	0.05	100
9	0.42	486	1.97	241	28	0.31	176	0.10	362
10	0.38	429	1.06	294	29	0.35	154	0.75	101
11	0.92	197	0.97	221	30	0.27	312	1.02	143
12	0.40	280	1.30	182	31	0.11	441	0.10	512
13	0.47	231	1.80	123	32	0.18	378	0.20	371
14	0.29	185	1.30	104	33	0.13	663	1.69	200
15	0.56	118	0.05	441	34	0.58	306	0.26	476
16	0.25	400	0.82	254	35	0.43	185	0.36	235
17	0.08	182	0.35	100	36	0.10	100	0.05	157
18	0.06	100	0.05	100	37	0.16	322	0.14	398
19	0.05	100	0.05	100	38	0.14	326	0.15	371

Since, IG is unstable for fault in five buses of network (1, 9, 10, 11, and 14) according to Table II, the lines of network can be divided into three groups. First group consist of lines that are not connected to unstable buses. The voltage drop in the terminal of IG is greater than CVS for the fault in all over these lines. Hence, it is not required to consider these lines in the stability constraints. Second group includes four lines within unstable buses (i.e. L10, L11, L13 and L15), and third group contains six other

lines, which are connected to unstable buses from one side (L1, L2, L9, L16, L17 and L19).

The faults on lines of groups 2 and 3 maybe cause to instability of IG. To prevent instability of IG, the setting of OCR relays on these lines are determined according to stability constraint. For example, relays R30 and R29 are located on lines L11 (group 2) and L10 (group 3), respectively. Fig. 7(a) shows the operating time of R30 for fault in L11 without considering CCT. According to Eq. (27), the relay curve is between upper relay curve (URC) and lower relay curve (LRC), depending on the fault location and resistance. The minimum margin between CCT and URC, without considering CCT constraint, is obtained 0,07. It can be seen from Fig.7(b), after applying the new method, the discrimination time between the CCT of IG and the operating time of OCR (URC) is greater than $CTI_2=0.2$ for the faults on different locations of the line.

It should be noted that, from Fig. 7(a), the voltage of IG (U_s) for the faults without resistances is in the range of $U_1=0$ to $U_2=0.11$. The constraint between two curves is satisfied in this range. However, U_s is in the range of 0 to $CVS=0.72$, with considering fault resistance, which the margin is lower than CTI_2 . Hence, the efficiency of new method which is based on IG terminal voltage, can be approved.

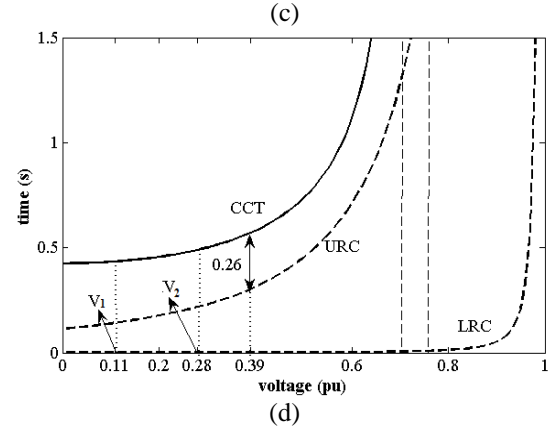
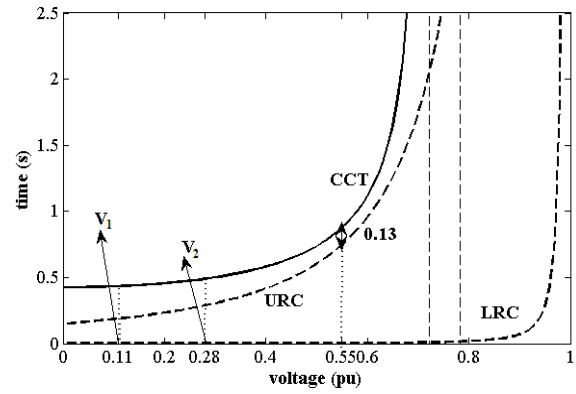
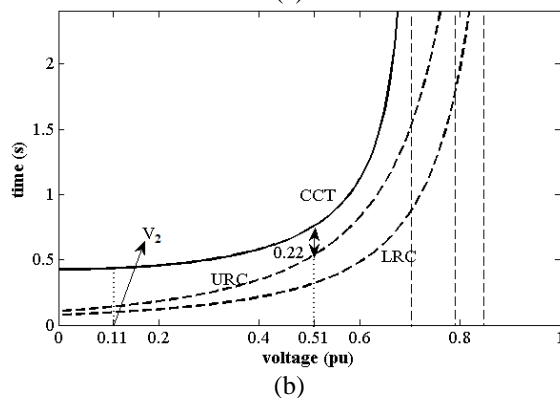
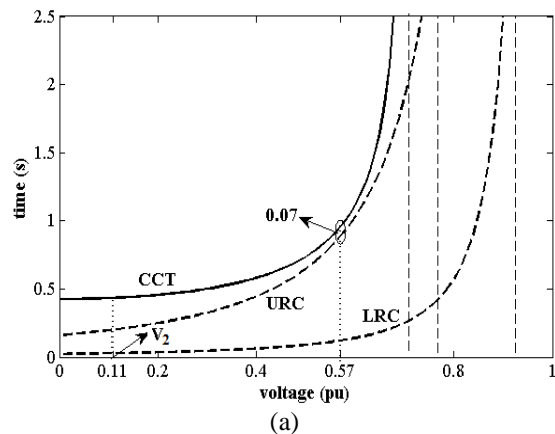


Fig. 5. Relay operating curves and CCT curves for fault throughout the lines. (a) Operation of R30 for fault in L11 without considering CCT. (b) Operation of R30 for fault in L11 with considering CCT. (c) Operation of R29 for fault in L10 without considering CCT. (d) Operation of R29 for fault in L10 with considering CCT.

5) Conclusion

In this paper, a terminal voltage based method is proposed for stability study of IG. To achieve this goal analytical method for CCT calculation is used for fault in all buses and lines of grid. The electrical torque of IG calculated as a function of rotor slip using the equivalent circuit of IG and network. Then, a new model is derived for representing the relation of CCT versus terminal voltage. the model is used to formulate OCR coordination algorithm considering stability constraints. By optimizing the pickup current of relays the appropriate curve of relay is selected proportional to CCT curve to satisfy the stability constraint. The proposed method is applied to two samples network and the results demonstrate the accuracy of new analytical method for CCT calculation. Also, the results show the efficiency of the new coordination algorithm in considering the stability of IG.

References

- [1] O. Samuelsson, S. Lindahl, "On speed stability", *IEEE Transactions on Power Systems*, vol. 20, no. 2, pp. 1179-1180, 2005.
- [2] J. Pedra, F. Corcoles, "On fixed-speed WT generator modeling for rotor speed stability studies", *IEEE Transactions on Power Systems*, vol.27, no. 1, pp. 397-406, 2012.

- [3] DJ. Trudnowski, A. Gentile, "Fixed-speed wind-generator and wind-park modeling for transient stability studies", *IEEE Transactions on Power Systems*, vol. 19, no. 4, pp. 1911-1917, 2004.
- [4] SK. Salman, ALJ. Teo, "Windmill modeling consideration and factors influencing the stability of a grid-connected wind power-based embedded generator", *IEEE Transactions on Power Systems*, vol. 18, no. 2, pp. 793-802, 2003.
- [5] HR. Najafi, F. Robinson, F. Dastyar, AA. Samadi, "Transient stability evaluation of wind farms implemented with induction generators", In 43rd International Conference on Universities Power Engineering (UPEC), December 2008, Padua, Italy, pp. 1-5.
- [6] R. Dashti, A. Vahedi, "Transient analysis of induction generator jointed to network at balanced and unbalanced short circuit faults", In 42nd International Conference on Universities Power Engineering (UPEC), September 2007, Brighton, UK, pp. 102-108.
- [7] T. Senjyu, N. Sueyoshi, "Stability analysis of grid connected wind power generating system", In *Third International workshop on Transmission Networks for offshore wind farms, 2002*.
- [8] SK. Salman, ALJ. Teo, "Investigation into the estimation of the critical clearing time of a grid connected wind power based embedded generator", In Transmission and Distribution Conference and Exhibition (TDC), October 2002, Yokohama, Japan, pp. 975-980.
- [9] T. Senjyu, N. Sueyoshi, K. Uezato, K. Fujita, A. Funabashi, "Transient stability analysis of induction generator using torque-time characteristic", In Fifth International Conference on Power Electronics and Drive Systems (PEDS), November 2003, Singapore, pp. 760-765.
- [10] P. Ledesma, J. Usaola, JL. Rodriguez, "Transient stability of a fixed speed wind farm", *Renewable Energy*, vol. 28, no. 9, pp. 1341-1355, 2003.
- [11] YJ. Lin, "Comparison of speed and voltage based critical clearing time of squirrel cage induction generator", In 11th International Conference on Probabilistic Methods Applied to Power Systems (PMAPS), June 2010, Singapore, pp. 283-286.
- [12] N. Amutha, BK. Kumar, "Effect of modeling of induction generator based wind generating systems on determining CCT", *IEEE Transactions on Power Systems*, vol. 28, no. 4, pp. 4456-4464, 2013.
- [13] N. Zhou, P. Wang, Q. Wang, PC. Loh, "Transient stability study of distributed induction generators using an improved steady-state equivalent circuit method", *IEEE Transactions on Power Systems*, vol. 29, no. 2, pp. 608-616, 2014.
- [14] H. Li, B. Zhao, C. Yang, HW. Chen, Z. Chen, "Analysis and estimation of transient stability for a grid-connected wind turbine with induction generator", *Renewable Energy*, vol. 36, no. 5, pp. 1469-1476, 2011.
- [15] Ap. Grilo, A. Mota, L. Mota, W. Freitas, "An analytical method for analysis of large-disturbance stability of induction generators", *IEEE Transactions on power systems*, vol. 22, no. 4, pp. 1861-1869, 2007.
- [16] AP. Grilo, MBC. Salles, FCL. Trindade, W. Freitas, "An analytical insight into large-disturbance stability of doubly fed induction generators", *Electric Power Systems Research*, vol. 122, pp. 29-32, 2015.
- [17] PK. Naik, NKC. Nair, AK. Swain, "Impact of reduced inertia on transient stability of networks with asynchronous generation", *International Transactions on Electrical Energy Systems*, vol. 26, no. 1, pp. 175-191, 2016.
- [18] MG. Maleki, RM. Chabanloo, H. Javadi, "Method to resolve false trip of non-directional overcurrent relays in radial networks equipped with distributed generators", *IET Generation, Transmission & Distribution*, vol. 13, no. 4, pp. 485-494, 2019.
- [19] LH. Chen, "Overcurrent protection for distribution feeders with renewable generation", *International Journal of Electrical Power & Energy Systems*, vol. 84, pp. 202-213, 2017.
- [20] D. Yoosefian, RM. Chabanloo, "Protection of distribution network considering fault ride through requirements of wind parks", *Electric Power Systems Research*, vol. 178, pp. 106019, 2020.
- [21] M. Nasiri, J. Milimonfared, SH. Fathi, "A review of low-voltage ride-through enhancement methods for permanent magnet synchronous generator based wind turbines", *Renewable and Sustainable Energy Reviews*, vol. 47, pp. 399-415, 2015.
- [22] R. Razzaghi, M. Davarpanah, M. Sanaye-Pasand, "A novel protective scheme to protect small-scale synchronous generators against transient instability", *IEEE Transactions on Industrial Electronics*, vol. 60, no. 4, pp. 1659-1667, 2013.
- [23] H. Yazdanpanahi, W. XU, "Contribution of induction-machine distributed generators to fault current and assessing their impact on overcurrent protection", In *26th Annual IEEE Canadian Conference on Electrical and Computer Engineering (CCECE), May 2013*, Regina, SK, Canada, pp. 1-4, 2013.
- [24] XF. Wang, Y. Song, M. Irving, "Modern power systems analysis", Springer Science & Business Media, 2010.
- [25] R. Mohammadi, AH. Abyaneh, HM. Rudsari, HF. Fathi, H. Rastegar, "Overcurrent relays coordination considering the priority of constraints", *IEEE Transactions on Power Delivery*, vol. 26, no. 3, pp. 1927-1938, 2011.
- [26] MR. Asadi, AH. Abyaneh, M. Mahmoodan, RA. Naghizadeh, A. Koochaki, "Optimal overcurrent relays coordination using genetic algorithm", in 11th International Conference on Optimization of Electrical and Electronic Equipment (OPTIM), May 2008, Brasov, Romania, pp. 197-202.
- [27] SA. Hosseini, H. Askarian Abyaneh, SHH. Sadeghi, F. Razavi, "Merging the retrieval of the protection coordination of distribution networks equipped with DGs in the process of their siting and sizing", *Journal of Emerging and Selected Topics in Power Electronic*, vol. 8, no. 3, pp. 035502, 2016.
- [28] N. Abdolghani, J. Milimonfared, MH. Zamani, "Improving Transient Stability of Dual Stator-Winding Induction Generator Based-Wind farms By Slip Frequency Control", *IEE Journal of Emerging and Selected Topics in Power Electronics*, vol. 9, no. 5, pp. 5354-5366, 2021.
- [29] D. Baimel, N. Chowdhury, J. Belikov, "New type of bridge fault current limiter with reduced power losses for transient stability improvement in DFIG wind farm", *Journal of Electric Power System Research*, vol. 197, pp. 107293, 2021.
- [30] HR. Shabani, M. Kalantar, A. Hajizadeh, "Investigation of the closed-loop control system on the DFIG dynamic models in transient stability studies", *International journal of Electrical Power and Energy Systems*, vol. 131, pp. 107084, 2021.

6) Appendix

The parameters of IGs in two case studies are listed in Table IV and also, transformer's parameters are listed in Table V. The line impedances in the simple network are:

$$Z_{L1} = Z_{L2} = Z_{L3} = 0.12 + j0.3\Omega$$

The capacity of load1 and load2 are 2MW and 1MW, respectively.

Table IV. The parameters of IGs in the sample networks

parameters	Simple network	IEEE 30bus
capacity	2MVA	1MVA
voltage	690v	11kv
R_s	0.048 p.u	0.04 p.u

X_s	0.075 p.u	0.08 p.u
R_r	0.018 p.u	0.024 p.u
X_r	0.13 p.u	0.14 p.u
X_m	3.8 p.u	3.67 p.u
H	1.5s	1.06s
X_c	4 p.u	4 p.u

Table V. The parameters of transformers in the sample networks.

parameters	Simple network	IEEE 30bus
capacity	3MVA	1.25MVA
R_T	0.02 p.u	0.01 p.u
X_T	0.1 p.u	0.05 p.u